Iraqi Journal for Applied Science (IJAS)
Vol. 1, No. 2, September, 2024, pp. 66-76
ISSN: 3006-5828, DOI:10.69923/ajdjnb33

Examining Metal Complexes Formed from New Schiff Base Ligand Derived from Benzene Carbaldehyde: Evaluation of Anti-biofilm and Anti-bacterial Properties

Enass J. Waheed
Department of Chemistry, College of Education for Pure Sciences, Ibn -Al-Haitham, University of Baghdad, Baghdad, Iraq.

Article Info

Article history:

Received: 01, 07, 2024
Revised: 29, 08, 2024
Accepted: 10, 09, 2024
Published: 30, 09, 2024

Keywords:

Benzene carbaldehyde,
Schiff base,
Antibiofilm,
Antibacterial

ABSTRACT

One of the most difficult tasks in modern medical societies is the process of identifying a cure for many infectious diseases caused by drug-resistant microbes. Therefore, it has become necessary to discover new compounds that work in this regard. The currently prepared Schiff base, derived from thiazole, has a biological activity against bacteria and biofilms and its activity increases when it is associated with copper, zinc and platinum ions and forms metal complexes. This study highlights the synthesis and evaluation of novel biological compounds as inhibitors of bacterial growth and biofilms. A three newly complexes are resulting from the reaction of a new Schiff base ligand (L_C) with metal ions (Zn, Cu, Pt). The new ligand (L_C) was prepared from the reaction of precursor (P) and benzenecarbaldehyde. The prepared compounds were characterized by $^{1}H\&^{13}CNMR$, FTIR, UV-Vis, Magnetic susceptibility, CHNS and Molar conductivity. It was determined that the anti-bacterial activity of the newly synthesized Lc and (Cu-Lc) was mightily significant towards more antibiotic-resistant bacteria and had low (MIC) values. Like that, anti-biofilm inhibitory of the same compounds showed 100% of clinical isolates of *P. aeruginosa* and *S. aureus* in 16 and 32 mg/ml respectively, whereas (Zn-Lc) were inhibited 100% in 4 mg/ml. On the other hand (Pt-Lc) inhibited 100 % in 2 mg/ ml. Good yield was obtained from the synthesis of new compounds from the starting material. They can be potential candidates as inhibitors of bacteria and biofilms.

Corresponding Author:

Enass J. Waheed
Department of Chemistry,
College of Education for Pure Sciences,
Ibn -Al-Haitham, University of Baghdad,
Baghdad, Iraq.
Email: enass.j.w@ihcoedu.uobaghdad.edu.iq

1. INTRODUCTION

S. aureus (G^+) and *P. aeruginosa* (G^-) are the causative agents of many prevalent and well-known human diseases and can colonize a wide range of sites with serious clinical consequences. The most common infections are among immuno compromised patients in hospitals, and are caused by infections resulting from burns, respiratory infections and cystic fibrosis [1-2]. One of the reasons for the spread and prosperity of these microorganisms is their ability to form biofilms and a large group of virulence factors related to the outside of the cell and the cell itself, and through transcriptional regulators they are controlled, which makes them adapt quickly to host defenses and environmental changes [3]. Biofilms are defined as a thin layer of living material that can form on nonliving surfaces such as metals, dead organisms, and air-water interfaces, as well as on living surfaces such as plants and animals. Biofilms contain homogeneous or heterogeneous bacterial communities embedded in a matrix of extracellular polymeric substances composed mainly of polysaccharides, in addition to proteins, lipids, and nucleic acids that can be found in this composition.

Biofilms pose a pathological risk and contribute to the occurrence of various pathological infections, in addition to their presence on the surfaces of medical equipment such as catheters, and facilitate the process of gene transfer between bacterial cells, which leads to an increase in the number of virulent strains on the one hand, and on the other hand, these same cells can evade host defenses and resist antibiotics, as the matrix composed of extracellular polymeric substances hinders the diffusion of antibiotics through the biofilm. Biofilm formation begins with the attachment of floating microorganisms to a surface. Initially, the first colonies adhere to the surface by weak, reversible van der Waals forces [4-6]. If colonies are not removed from a surface promptly, they can become permanently attached by cell adhesion molecules such as bacterial cilia. Early colonizers facilitate the access of other cells by providing different types of attachment sites and building an extracellular matrix that holds the biofilm together. Some species cannot attach to a surface on their own, but can attach to the extracellular matrix or directly to early colonizers. When invading a surface and forming a biofilm, cells communicate by quorum sensing. Once invasion has occurred, the biofilm gradually grows by cell division and recruitment of new cells. The final stage of biofilm formation is called development, and it represents the stage in which the biofilm is fully established. At this stage, the biofilm can only change in shape and size. Development of the biofilm allows cells to become more resistant to antibiotics [7,8]. In this context and due to the large history of metal compounds with antimicrobial properties, drugs based on zinc, platinum, and copper have been widely evaluated [9]. Benzene carbaldehyde is an organic compound with the chemical formula (C_6H_5CHO) containing of a C_6H_6 ring and a substituted (formyl) group. It is the simplest and most useful aromatic aldehyde in industrial fields. In 1832, the Friedrich and Justus were able to synthesize benzaldehyde for the first time [10]. The goal of the study is to prepare new Schiff base complexes resulting from the binding of the new ligand (L_C) with metal ions Pt(IV), Zn(II) and Cu(II) and then test their biological activity represented by antibacterial and antibiofilm activity towards clinically relevant strains based on the minimum inhibitory concentration (MIC) method.

2. METHOD

Materials and instruments

All chemicals and solvents (sulfuric acid, cefixime, glacial acetic acid, absolute ethanol, HCl, benzene, carbaldehyde, methanol, diethyl ether, zinc chloride, copper (II) chloride dihydrate, potassium hexachloroplatinate, sodium chloride) are supplied by certified companies (BDH, Merck, Fluka) with a high degree of purity.

Measurement of electronic transfers of compounds prepared at laboratory temperature and with a quartz cell (1cm) was carried out using a device UV-M90 Double Beam Spectrophotometer. Analysis of microelements (CHNS) was performed using a device Euro EA CHNSO Elemental Analyzer. Infrared spectroscopy was performed for the prepared compounds within the range (4000–400) cm^{-1} with potassium bromide tablets using a device Shimadzu FTIR-8400S Spectrometer. Electrical conductivity measurement was performed at concentration (10^{-3} M) and laboratory temperature with DMSO solvent by a Philips pw-Digital Meter conductance. The atomic absorption measurement of the syntheses compounds was carried out using a device Shimadzu AA-7000 Shimadzu. An examination of the magnetic susceptibility of metal complexes was carried out at 25 °C by a device the Sherwood Scientific's Magnetic Susceptibility Balances. ^{1}H, ^{13}C NMR spectroscopic measurements of the prepared ligand was performed using a device Bruker AVANCE NEO 400 MHz spectrophotometer with DMSO. Determination of chlorine content in the prepared compounds was carried out using 686-Titro processor – 665 Dosimat. Metrohm. Swiss.

Synthesis of New Schiff base ligand [ethyl (6R ,7R) -7- ((E) -2- (2- (((E) -benzylidene) amino) thiazol -4-yl) -2- ((2- ethoxy -2- oxo ethoxy) imino) acetamido) -8- oxo -3- vinyl -5-thia -1- aza bicyclo [4.2.0] oct -2- ene -2- carboxylate] (L_C)

Prepare ligand (L_C) in two steps:-

A. Synthesis of precursor (P)

Using a 100mL round flask, (0.47g, 1mmol) of cefixime was dissolved in (1mL) of absolute ethanol containing dissolved HCl, where saturated absolute ethanol was prepared. With HCl gas, by adding an amount of concentrated sulfuric acid to a flask containing an amount of sodium chloride (NaCl), and we collect the liberated gas in a flask containing ethanol, which is formed (ethanol saturated with HCl gas) and the mixture is left to stir continuously. With reflux for 3 hours, the course of the reaction was followed by TLC. After that, the mixture was cooled to obtain ester crystals and they were recrystallized using hot methanol and diethyl ether. The percentage of the product after drying the precipitate was 85% and its melting points were (109-111°C) [14].

B. Synthesis of (L_C) New Schiff base Ligand

The New Schiff base ligand (L_C) was prepared by adding a solution of the substance obtained in the first step (P) (0.51g, 1mmol) in 10 mL of ethanol to a solution of benzene carbaldehyde (0.11g, 1mmol in 10 mL of ethanol with the addition of 3-4 drops of glacial acetic acid. After stirring for one hour, the mixture was placed for 3 hrs (under reflux), and then the course of the reaction was followed by TLC.After that, the mixture was filtered to obtain the desired precipitate (orange), and the precipitate was recrystallized using hot methanol and diethyl ether. The precipitate was then left to dry at room temperature and was weighed to calculate the percentage of the product, which was (74%). And the melting point is (196-198) °C [15], Scheme 1.

Synthesis of the complexes

The zinc complex was prepared with a molar ratio of (1:1) (M:L) using a 100mL round flask by adding (0.14gm) (1mmol) of ($ZnCl_2$) dissolved in (10mL) ethanol to the ligand solution (L_C) resulting from dissolving (0.59gm, 1mmol) in (10mL) ethanol and leave the mixture at a temperature of 70 °C with continuous stirring and reflux for (3 hours). Filter the solution to obtain the yellow precipitate. It was washed several times with H_2O distilled and $(C_2H_5)_2O$ and re-crystallized with CH_3OH absolute. Then the percentage of the product, which was (68%), and the melting point (211-213)°C were calculated. Preparation of the remaining complexes M= Pt(IV) and Cu(II) of the ligand (L_C), these complexes were prepared by the same method mentioned [16], Scheme 1.

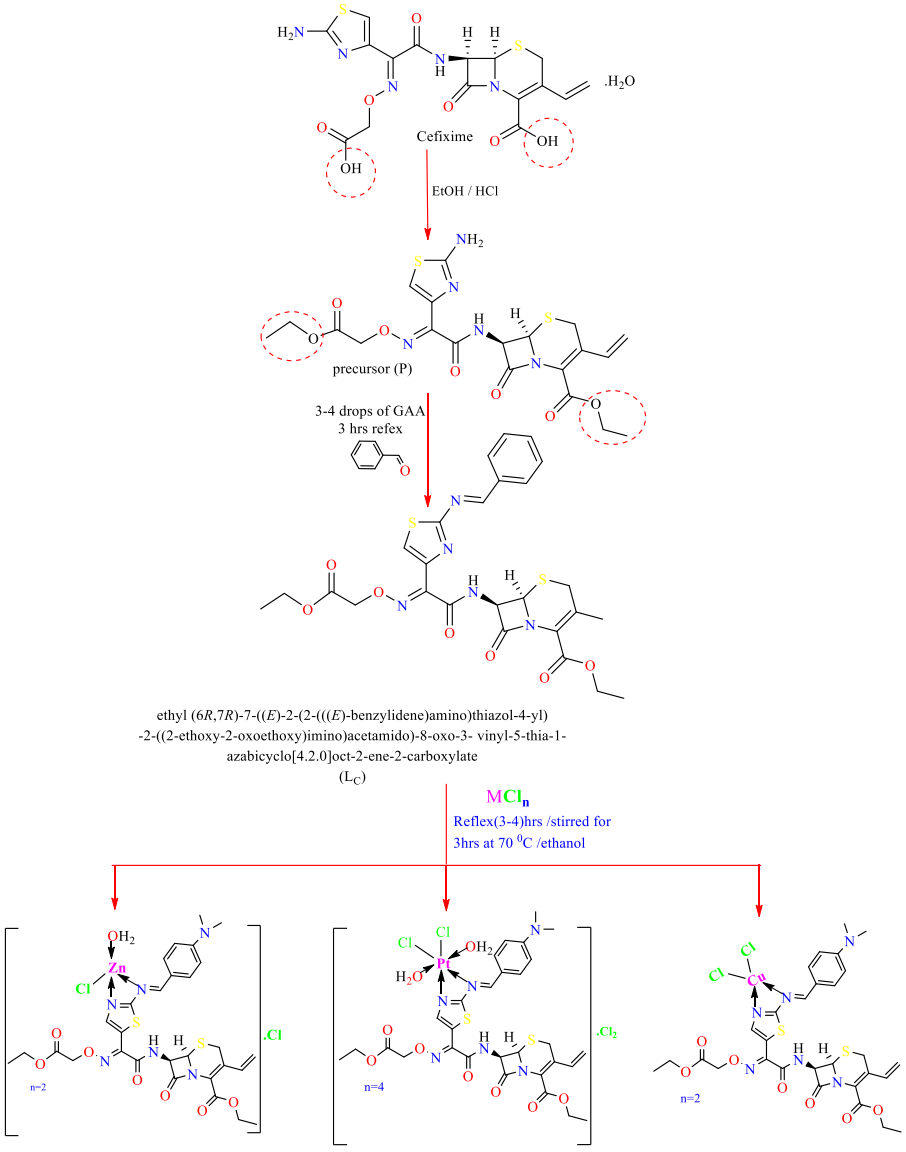

Scheme1: Synthesis of ligand (L_C) and its complexes

Biofilm and antibacterial information

The culture was grown overnight in TSB supplemented with 1% glucose after *S. aureus* and *P. earuginosa* had been revived on blood agar plates. To achieve an optical density at 600 nm (OD600) of ~0.1, the overnight culture was diluted 1:50 in TSB and 2% glucose. In addition to 100 µl of Lc and its complexes in each well of a 96-well plate, 100 µl of the diluted basal culture was drained, resulting in a final volume of 200 µl per well. Incubation was carried out at 37°C under static conditions for 18 h after which only sterile liquid medium covered with its three coverslips (as a control) was used. To remove unattached bacteria after incubation, planktonic cells were rinsed twice with distilled water. After that for 20 min at room temperature, the adherent bacterial cells in each well were fixed with 200 µl of absolute methanol. Then the adherent cells were stained by adding 200 µl of 0.1% crystal violet to each well for 15 min. Using DW, the excess dye was removed by washing it repeatedly. To ensure complete dryness, the plate was dried in the room for 30 min. In the final stage, to fix the dye, 33% acetic acid was added. Using an automatic ELISA reader, the biofilm was evaluated by determining the (OD) optical density readings at 630 nm (wavelength) [11].

Biofilm reduction %= (OD630nm of bio film growth control – OD630nm of treated isolate)/ OD630nm of bio film growth control×100.

Minimum inhibitory concentration (MIC)

The both micro dilution method was performed for test material determination:

1- Preparation of test material
2- Dilution of 1\10 in a sterile mullar hinton broth (MHB).
3- Transfer 100 microliters of diluted test material to the first line of wells.
4- Add 100 microliters of broth medium in each well from 2 to 12.
5- Two fold dilution: by transferring 100 microliters from the first to the 10th well
6- Except well 11 and 12 were used as controls (positive & negative).
7- All wells were inculcated with 20 microliters of bacterial suspension comparable to McFarland standard no 5 ($1.5 * 10^8$ CFU\ml).
8- The microtitre plate was incubated at 37 ^{0}C (24 h).
9- The MIC value was determined the lowest concentration that inhibits bacteria growth. The growth was measured at OD_{450} determination using a microtiter plate reader [12].

Antibacterial activity assay

For the purpose of testing the ability of the synthesized compounds to inhibit the selected bacteria, the diffusion method was used. By steam sterilization at 121 °C for 15 minutes, the prepared what man filter paper discs with a diameter of 6 mm No. 3 were sterilized, then 100 µg of the synthesized compounds were placed on each disc, followed by placing the discs on the upper surface of the culture plate [13].

3. RESULTS AND DISCUSSION

Some physical properties of the synthesized compounds were determined, including complex colors, thermal stability, elemental analysis, metal content determination, and matching the calculated values with the experimental results, Table 1.

Table 1: Analytical data of synthetic compounds

Com.	Colour	M . wt	m . p	Calculated (Actual)					
				%M	%C	%H	%N	%S	%Cl
Ligand (L_C)	Orange	585.65	196-198 ^{0}C	-	53.60 (53.32)	4.72 (4.65)	12.00 (11.96)	10.82 (10.95)	-------
$[Cu(L_C)Cl_2]$	Olive	775.18	252-254 ^{0}C	8.13 (8.20)	45.00 (44.93)	4.21 (4.16)	10.91 (10.84)	8.24 (8.27)	9.11 (9.15)
$[Pt(L_C)(H_2O)_2Cl_2].Cl_2$	Turmeric	1013.64	270-272 ^{0}C	19.33 (19.25)	34.23 (34.36)	3.71 (3.58)	8.15 (8.29)	6.25 (6.33)	13.47 (13.99)
$[Zn(L_C)(H_2O)Cl].Cl$	Yellow	794.02	211-213 ^{0}C	8.19 (8.23)	43.78 (43.87)	4.15 (4.19)	10.39 (10.58)	8.12 (8.08)	8.67 (8.93)

^{1}H,^{13}CNMR spectra

The Proton NMR spectral data of ligand L_C is listed in Table 2, Figure 1 [22].

Table 2: Proton NMR data for ligand with DMSO-d6

Ligand	Protons Type	Protons number	δ (ppm)
L_C	6H, proton $2CH_3$ group	H11	0.88-1.74
	4H, proton $2O-CH_2$ group	H10	3.43-3.48
	4H, proton $S-CH_2$ + $O-CH_2$ group	H4, H26	3.84-4.46
	5H, proton C-H group	H6, H7, H12, H13	4.88-5.31
	5H, proton C-H $_{aromatic}$ group	H23, H24 , H25	6.77-7.97
	1H, proton NH group	------	8.15
	1H, proton N=CH group	H21	8.58
	1H, proton C=CH-S group	H20	10.03

The Carbon NMR data of ligand L_C is listed in Table 3, Figure 1 [23].

Table 3: Carbon NMR data for ligand with DMSO-d6

Ligand	Carbons Type	Carbons number	δ (ppm)	Carbons Type	Carbons number	δ (ppm)
L_C	2C, CH_3	C11	19.02	1C,CH aromatic	C22	131.19
	1C, $S-CH_2$	C4	29.85	1C,C aromatic	C25	133.34
	1C, N-CH	C7	56.49	1C,=C	C3	135.07
	2C,$O-CH_2$	C10	61.19	1C,=C	C19	136.62
	1C,S-C-N	C6	64.33	1C,C=N	C15	157.63
	1C,$NOCH_2$	C26	71.96	1C,C=N	C21	161.53
	1C,$=CH_2$	C13	115.50	1C,NHCO	C14	164.16
	1C,N-C=	C2	126.63	1C,NC=O	C8	165.58
	1C,S-CH=	C20	128.96	1C,OC=O	C9	167.78
	2C,CH aromatic	C23	129.04	1C,OC=O	C27	169.74
	1C,=CH	C12	129.63	1C,N=C-N	C17	175.26
	2C,CH aromatic	C24	129.97			

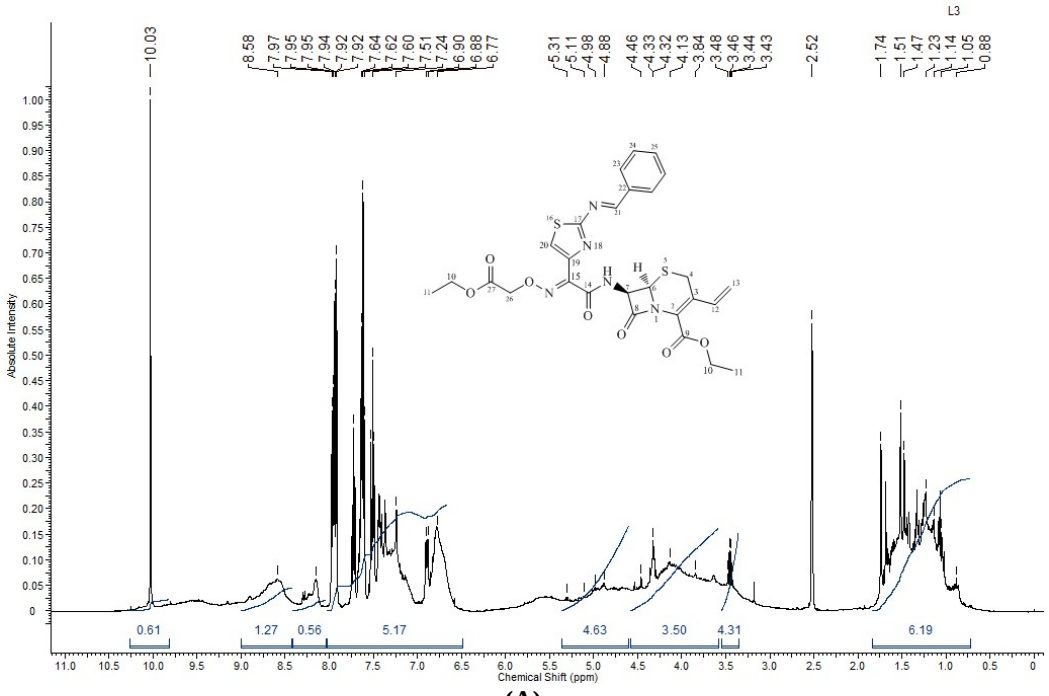

(A)

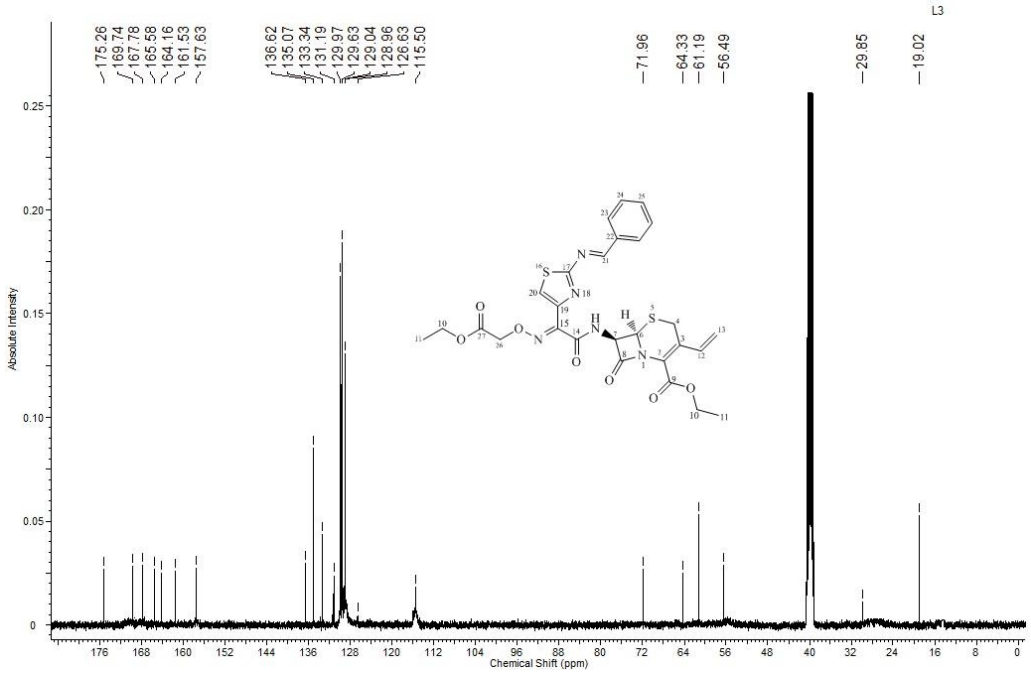

(B)

Figure 1: ^{1}H (A),^{13}C(B)-NMR spectrum of ligand L_C

FT-IR spectrum of (L_C) and its complexes

In Table 4, the ligand (L_C) was identified by studying its infrared spectrum shown in Figure 2, where strong band at (3237) cm^{-1} cm was observed, is attributed to the frequency $\upsilon(N–H)_{str.}$ As for the two sharp, strong bands at wave numbers (1747) cm^{-1} and (1697) cm^{-1}, they are attributed to the stretching frequency bands of the CO group υ $(C=O)_{ester}$ and $\upsilon(C=O)_{amide}$ respectively, with the appearance of other stretching frequency bands at (1593) cm^{-1}, (1516) cm^{-1} and (1230,1172)cm^{-1} belong to the aggregates υ $(C=N)_{five\ ring}$, $\upsilon(N\text{-}H)_{bend,}$ $\upsilon(C\text{-}O\text{-}C)_{ester}$ respectively and finally a band appears at the wave number (1651)cm^{-1} is due to $\upsilon(CH=N)_{imine}$ for (L_C)[17,18]. The prepared complexes were identified by following their infrared spectra and comparing them with the spectrum of the prepared ligand (L_C). It was observed that some bands shifted and new bands appeared while other bands remained stable. The infrared spectra of the metal complexes of the ligand showed (L_C) represented by Figure 1 is absorption bands within the range (3475-3225) cm^{-1}, (1747-1739) cm^{-1} and (1697-1685) cm^{-1} back to υ $(N–H)_{str.}$, $\upsilon(C=O)_{ester}$ and $\upsilon(C=O)_{amide}$ respectively, which did not participate in the coordination of the prepared complexes, while the coordination of the ligand (L_C) with the metal ions was revealed through absorption bands of the order of (1654-1639) and (1608-1597) cm^{-1} , which are back to the groups of $\upsilon(C=N)_{imine}$ and $\upsilon(C=N)_{five\ ring}$ respectively, which were shifted towards different frequencies compared to their absorption band in the free ligand (L_C). What enhances this consistency is the appearance of weak absorption bands in the range (582-466) and (556-420) cm^{-1} back to the υ(M-N) bands in the complexes. Which confirms the coordination of water with the central ion is the shower of bands in the range (840) cm^{-1} back to $\rho(H_2O)$ in the spectrum of $Zn^{(II)}$ and $Pt^{(IV)}$ complexes [19-21], Table 4.

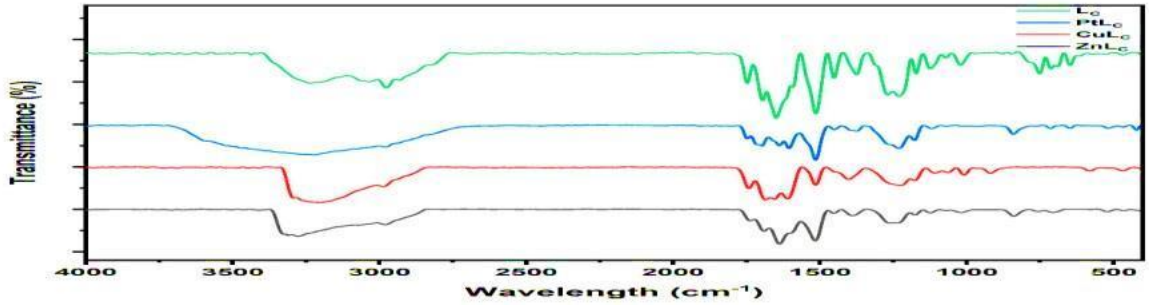

Figure 2: FTIR spectrum of L_C and its complexes

Table 4: FTIR data of ligand with complexes

Com.	υ (N-H)$_{str.}$ υ (N-H)$_{bend}$	υ (C=O) υ(C-O-C) ester	υ (C=N) five ring	υ (C=O) amide	υ (C=N) imine	ρ (H_2O)	υ(M - N) υ (M - N)
Ligand (L_C)	3237 1516	1747 1230 1172	1593	1697	1651	_____	—— ——
[Cu(L_C)Cl_2]	3475 3414	1743 1222 1176	1608	1685	1654		**582** **456**
[Pt(L_C)(H_2O)$_2$$Cl_2$].$Cl_2$	3225 1516	1747 1230 1176	1604	1697	1639	480	**466** **420**
[Zn(L_C)(H_2O)Cl].Cl	3471 1516	1739 1234 1176	1597	1693	1639	480	**466** **424**

Electronic spectra

All electronic transition data for the spectra of the synthesized compounds [24,25] are included in the table 5 and Figure 3.

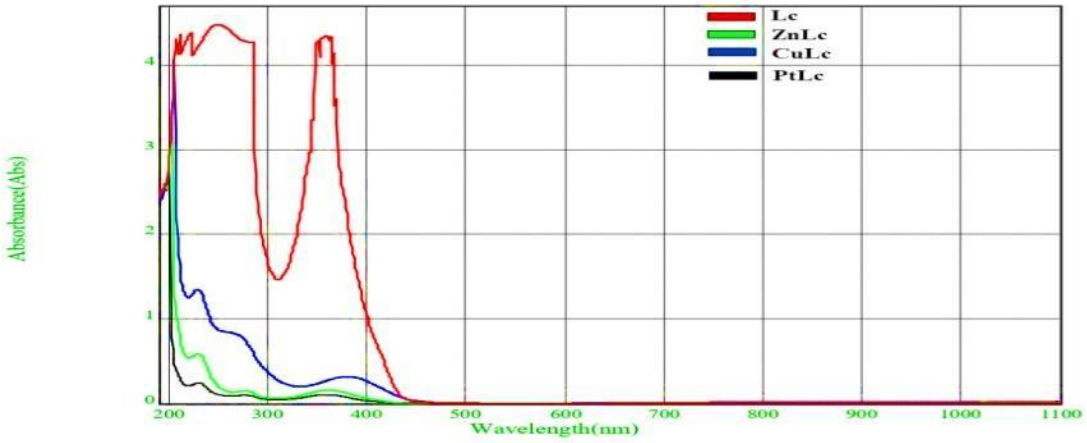

Figure 3: Electronic spectrum of the synthesized compounds

Table 5: UV/Vis data of ligand with complexes.

Compound	Maximum absorption υmax(cm^{-1}) and (nm)	Band assignment	Molar Conductivity (Electrolyte nature)	μ_{eff} (B.M)	Suggested geometry
Ligand (L_C)	36764(272)	$\pi \rightarrow \pi^*$	------	-------	-------
[Cu(L_C)Cl_2]	40485(247) 34722(288) 23529(425) 20833(480)	Intra Ligand Intra Ligand C.T $^2B_1g \rightarrow {}^2Eg$	16.50 **(Non-electrolyte)**	0	Square planer
[Pt(L_C)(H_2O)$_2$$Cl_2$].$Cl_2$	16077(622) 18867(530) 23923(418)	$^1A_1g \rightarrow {}^3T_1g$ $^1A_1g \rightarrow {}^3T_2g$ C.T	76.41 (**Electrolyte**)	0	Octahedral
[Zn(L_C)(H_2O)Cl].Cl	22471(445)	C.T	35.12 (**Electrolyte**)	0	Tetrahedral

CT = Charge of Transfer IL=Intra of Ligand

The table (6), show anti-biofilm activity of L_c, Cu-L_c, Zn-L_c and Pt-L_c on biofilm inhibition

Table 6: Before and after treatment with (L_C, Cu-L_C, Zn-L_C, Pt-L_C) biofilm formation of clinical isolates of *P. aeruginosa* and *S. aureus*.

No of isolates	Before treatment	After treatment concentration (L_C)							
		128	64	32	16	8	4	2	1
S_{a-1}	+++	-	-	-	-	-	+	++	++
S_{a-2}	+++	-	-	-	-	-	+	++	++
S_{a-3}	+++	-	-	-	-	-	-	-	++
S_{a-4}	+++	-	-	-	-	-	+	+	++
S_{a-5}	+++	-	-	-	-	-	+	+	++
P_{a1}	+++	-	-	-	-	+	++	++	+++
P_{a-2}	+++	-	-	-	-	+	+	++	++
P_{a-3}	+++	-	-	-	+	+	++	+++	+++
P_{a-4}	+++	-	-	-	+	+	+	+	++
P_{a-5}	+++	-	-	-	-	+	+	++	++
No of isolates	**Before treatment**	**After treatment concentration (Cu-L_C)**							
		128	64	32	16	8	4	2	1
S_{a-1}	+++	-	-	-	-	-	+	+	+
S_{a-2}	+++	-	-	-	-	+	+	+	+
S_{a-3}	+++	-	-	-	-	-	+	++	++
S_{a-4}	+++	-	-	-	-	+	+	++	++
S_{a-5}	+++	-	-	-	-	-	+	+	++
P_{a1}	+++	-	-	-	-	+	+	+	++
P_{a-2}	+++	-	-	-	++	++	++	++	++
P_{a-3}	+++	-	-	-	-	-	+	+	+
P_{a-4}	+++	-	-	-	-	++	++	++	++
P_{a-5}	+++	-	-	-	-	++	++	++	++
No of isolates	**Before treatment**	**After treatment concentration (Zn-L_C)**							
		128	64	32	16	8	4	2	1
S_{a-1}	+++	-	-	-	-	-	-	++	++
S_{a-2}	+++	-	-	-	-	-	-	++	+
S_{a-3}	+++	-	-	-	-	-	-	++	+++
S_{a-4}	+++	-	-	-	-	-	-	+	+
S_{a-5}	+++	-	-	-	-	-	-	++	++
P_{a1}	+++	-	-	-	-	-	-	+	++
P_{a-2}	+++	-	-	-	-	-	-	-	+
P_{a-3}	+++	-	-	-	-	-	-	++	++
P_{a-4}	+++	-	-	-	-	-	-	++	++
P_{a-5}	+++	-	-	-	-	-	-	+++	+++
No of isolates	**Before treatment**	**After treatment concentration (Pt-L_C)**							
		128	64	32	16	8	4	2	1
S_{a-1}	+++	-	-	-	-	-	-	-	++
S_{a-2}	+++	-	-	-	-	-	-	-	+
S_{a-3}	+++	-	-	-	-	-	-	-	+
S_{a-4}	+++	-	-	-	-	-	-	-	+
S_{a-5}	+++	-	-	-	-	-	-	-	++
P_{a1}	+++	-	-	-	-	-	-	-	+
P_{a-2}	+++	-	-	-	-	-	-	-	+
P_{a-3}	+++	-	-	-	-	-	-	-	++
P_{a-4}	+++	-	-	-	-	-	-	-	++
P_{a-5}	+++	-	-	-	-	-	-	-	++

(*Sa*): *S. aureus*, (*Pa*): *P. aeruginosa*, S= +++, M= ++, W= + and NBf= -

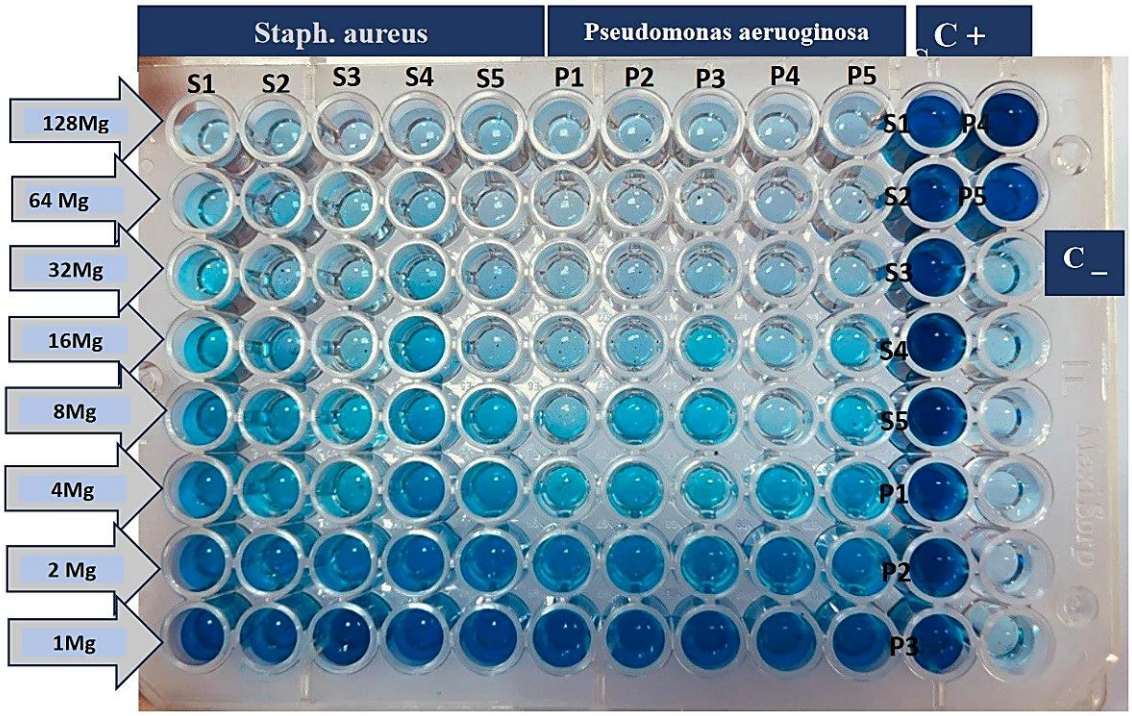

Figure 4 : Before and after treatment with of synthetic compounds biofilm formation of clinical isolates of *P. aeruginosa* and *S. aureus.*

The table (7), show antibacterial activity of L_c, Cu-L_c, Zn-L_c and Pt-L_c on selected bacteria

Table (7): Antibacterial activity of Lc and complexes compounds

Comp	Minimum Inhibitory Concentration in mg\ ml average of inhibition zone diameter (mm)	
	P.aeruginosa	*S.auerus*
Lc	8.15	9.12
Cu-L_C	10.4	10.7
Pt-L_C	10.6	11.2
Zn-L_C	11	11.8

MIC values were at concentration range, 32.64.128 mg\ ml

4. DISCUSSION

We need to understand how biofilms are formed in order to be able to synthesize and develop materials that can effectively inhibit or kill microbial growth and form biofilms. Over the past centuries, the formation of primary biofilms and the process of microbial attachment have been extensively studied. Biofilms can be described as an adherent swarm of living microorganisms that are assembled into a self-generated extracellular polymer (EPS) matrix [26], which in turn poses a serious threat in the fight against biofilm-related diseases as they build a barrier and protective layer that increases the resistance of encapsulated pathogens to antibiotics. Since bacterial strains contain cilia, extracellular DNA, binding proteins, flagella, and adhesive fibers [27]. This has led to the use of synthetic compounds of ligand and its copper complex to inhibit antibiofilm with 100% antibacterial activity against *S. aureus* and *P. aeruginosa* at concentrations 16 and 32 mg/ml, respectively, shown in (Table 6), while the zinc complex was used to inhibit the anti-biofilm activity against *S.aureus* and *P. aeruginosa* by 100% at 4 mg / ml, shown in (Table 6). A higher anti-biofilm activity against *S. aureus* and *P. aeruginosa* was observed when using the platinum complex compared to the ligand used alone and by 100% at 2 mg / ml, shown in (Table 6 and Fig.4). Surface conditioning (formation of a film composed of inorganic and organic molecules and nutrients absorbed on the surface) is the stage preceding cell attachment and biofilm formation. Surface conditioning is vital for cell growth, creating a favorable environment for bacterial attachment and then promoting cell adhesion to surfaces, causing infection [28]. Therefore, the presence of ligands and their complexes in growth media is considered to be an unfavorable condition that prevents cell attachment or can reduce surface adhesion. Based on their importance and biological roles, metals can be divided into two main categories, the first is

biologically relevant micronutrients such as iron, zinc, manganese, and copper, and the second is toxic-heavy metals. Therefore, most excess metal ions show toxicity by multiple mechanisms, including membrane and protein damage and generation of reactive oxygen species leading to antibiotic activity [29]. The inhibition ability of the synthetic compounds to the growth of bacteria represented by certain selected species was tested. They showed different inhibition abilities due to genetic differences and cell wall structure. The results obtained in this study showed that the synthetic compounds had a high inhibitory effect against Gram-positive bacteria (*S.aureus*) and a moderate inhibitory effect against Gram-negative bacteria (*P.aeruginosa*), where the inhibition rate of metal complexes was higher than that of the free ligand (Table 7). Researchers in previous studies, including Prakash et al. (2009) and Santhosh et al. (2010), obtained similar results, including high inhibition against Gram-positive bacteria compared to Gram-negative bacteria for compounds containing metal ions, and the results showed a mild response at concentrations of 50 and 100 μg/ml. The difference between G+ and G- bacteria is the chemical composition of the cell wall, as G+ bacteria contain fewer amino acids than G- bacteria and contain higher lipid content in G- bacteria than G+ bacteria. The cell wall in G+ bacteria is less complex than in G- bacteria, as the cell wall in G+ bacteria consists of two layers, which are the mucopeptide layer known as peptidoglycan and the second layer is composed of teichoic acid. As for the cell wall of G- bacteria, it consists of three layers, which are the mucopeptide layer known as peptidoglycan, a sugar lipid layer, and a protein lipid layer. The peptidoglycan layer of G- bacteria does not contain teichoic acid, but it does contain lipoproteins called mureins; these are important for linking the peptidoglycan layer to the outer envelope. The outer envelope contains lipopolysaccharides (LPS) that are important for causing heat in the host. The outer membrane contains porin proteins, which allow nutrients to enter, shown in (Table 7) [30].

5. CONCLUSION

This study summarizes the preparation of (L_C) resulting from the reaction of the intermediate (P) with the selected aldehyde (benzene carbaldehyde) as a first step, then the metal complexes are synthase from the reaction of the synthesized ligand with the mentioned metal ions as a second step, followed by the identification of the synthesized compounds by several spectroscopic methods to prove the geometric shapes of the metal complexes and finally the implementation of medical biological applications including anti-bacterial and anti-biofilm against specific bacterial strains *S. aureus* and *P. aeruginosa*, which clarified the possibility of using them in the future as therapeutic agents.

ACKNOWLEDGEMENTS

My thanks and gratitude to everyone who helped me completes this paper.

REFERENCES

[1] Ali, S., R. Delaramsadat, and R. Farzaneh, Evaluate the effect of zinc oxide and silver nanoparticles on biofilm and icaA gene expression in methicillin-resistant Staphylococcus aureus isolated from burn wound infection. Journal of Burn Care and Research, 2020. 1(6): p.1253-1259.

[2] Awf, A. R. and T. Ahmed, Synthesis, Characterization and Anticorrosion Studies of New Co(II), Ni(II), Cu(II), and Zn(II) Schiff Base Complexes. International Journal of Drug Delivery Technology, 2021. 11(2): p.414-422.

[3] Nils, H., D. Katharina, and S. Frederic, Anti-bioflm properties of laser-synthesized, ultrapure silver–gold-alloy nanoparticles against Staphylococcus aureus. Scientifc Reports, 2024. 14(34):p.1-15.

[4] Cheng, H., Q. Abdul, and K. See, Synthesis and Staphylococcus aureus biofilm inhibitory activity of indolenine-substituted pyrazole and pyrimido [1,2-b] indazole derivatives. Bioorganic & Medicinal Chemistry, 2023. 95:p.117-136.

[5] Thaer, S. and J. Enass, Synthesis, Spectroscopic Identification and Antimicrobial Activity of Mixed Ligand Complexes of New Ligand [3-((4- Acetyl Phenyl)Amino)-5,5-DimethylCyclohex-2-en-1-one] (HL*) With 3-Amino Phenol. Biochemical and Cellular Archives, 2020. 20(1): p.2235-2245.

[6] Dhekra, J. and G. Angham, Exploring the Biological Activity of Organotin Carboxylate Complexes with 4-Sulfosalicylic Acid. Bull. Chem. Soc. Ethiop, 2023. 37(6): p.1435-1442.

[7] Elena, Y., Y. Larisa, and R. Ekaterina, Synthesis, Antimicrobial and Antibiofilm Activities, and Molecular Docking Investigations of 2-(1H-Indol-3-yl)-1H-benzo[d]imidazole Derivatives. Molecules,. 28:p. 70-95.

[8] Uzma, J., K. Shoaib, and H.Rafaqat, In vitro and in silico correlation of bis-thiazole based Schiff base hybrids analogues: A computational approach develop to promising, cetylcholinesterase and butyrylcholinesterase inhibitors. Journal of Molecular Structure, 2024.13(3): p.137-150.

[9] Enass, J., Synthesis, Spectral and Thermal Characterization of Ni(II) ,Cu (II) and Zn(II) Complexes with New Ligand Towards Potential Biological Application. Biochemical and Cellular Archives, 2020. 20(1):p. 2483-2494.

[10] Joao, P., N. Ana, and M. Monica, Boroxine benzaldehyde complex for pharmaceutical applications probed by electron interactions. Rapid Commun Mass Spectrom, 2023. 37(1): p.e94-e118.

[11] Vogel, A. J. ,A Textbook of Practical Organic Chemistry. 3rd Edition, English Language Book Society and Longman Group Ltd., London, 1975: p.969-971.

[12] Eman, A. K., N. J. Hussien, and M.Y. Siti Fairus, Synthesis, Characterization and Antibacterial Activity of some New Metal Complexes Containing Semicarbazide. Iraqi Journal for Applied Science (IJAS), 2024. 1(1): p. 36-49.
[13] Aemin, A., P. Muhammad, and S. Zohaib, Synthesis and biological evaluation of 4-dimethylaminobenzaldehyde derivatives of Schiff bases metal complexes: A review. Inorganic Chemistry Communications, 2022. 145:p. 109-123.
[14] Jaffar, N., T. Miyazaki, and T. Maeda, Biofilm formation of periodontal pathogens on hydroxyapatite surfaces: Implications for periodontium damage. Journal of Biomedical Materials Research Part A, 2016. 104(11):p. 2873-2880.
[15] Hirakawa, H. and H. Tomita, Interference of bacterial cell-to cell communication: a new concept of antimicrobial chemotherapy breaks antibiotic resistance. Frontiers in microbiology, 2013. 4(114):p. 1-14.
[16] Irie, Y., K. Kragh, and V. Gordon, The Pseudomonas aeruginosa PSL Polysaccharide Is a Social but Noncheatable Trait in Biofilms. American society of microbiology, 2017. 8(3):p. e374-e387.
[17] Khalifa, O. and Waheed, E., Synthesis, spectroscopic characterization, molecular docking, antioxidant and anticancer studies of some metal complexes from tetraazamacrocyclic Schiff base ligand. Oncology and Radiotherapy, 2023. 17(11):p.244-257.
[18] El Mahmoudi, A., T. Anne-Sophie, and B. Magalie. Green synthesis and anti-biofilm activities of 3,5-disubstituted isoxazoline/isoxazole-linked secondary sulfonamide derivatives on Pseudomonas aeruginosa. Bioorganic & Medicinal Chemistry Letters, 2023. 96(15): p. 129-135.
[19] Wisam, A. and, A. Iman, Metal Complexes of Ligand Derived from Amine Compound: Formation, Spectral Characterization, and Biological Evaluation. International Journal of Drug Delivery Technology, 2021. 11(3):p. 728-734.
[20] Marwa, H. and M. May, Synthesis, Characterization, Molecular Docking, ADMET Study, and Antimicrobial Evaluation of New Mannich Bases of Isatin–Thiazole Imine Bases. Al-Rafidain J Med Sci, 2024. 6(2): p:201-208.
[21] Nawras, A. and J. Enass, Synthesis, Characterization, Thermal and Biological Study of New Organic Compound with Some Metal Complexes. International Journal of Drug Delivery Technology, 2021. 11(2): p.401-408.
[22] Heba, Y. J. and H. Mustafa, Synthesis, Green Chemistry Method Characterization of $CuFe_5O_8$ Nanocomposite and Assessment of Its Prostate Cancer-Preventive Effects. Iraqi Journal for Applied Science (IJAS), 2024. 1(1): p. 81-87.
[23] Davoodbasha, M., A. Kannappan, and L. Murugan, Unveiling the Anti-Biofilm Property of Hydroxyapatite on Pseudomonas aeruginosa: Synthesis and Strategy. Pharmaceutics, . 15(2):p.463-472.
[24] Tanzeela, Q., A. Saadat, and A. Mohammad, Design, synthesis, and unraveling the antibacterial and antibiofilm potential of 2-azidobenzothiazoles: insights from a comprehensive in vitro study. Sec. Organic Chemistry, 2023. 11:p.1-21.
[25] Walaa, H., B. Mahmoud, and M. El Mosallamy, Schiff base transition metal (II) complexes: spectral analyses and biological application. Egypt. J. Chem, 2024. 67(3): p.379-386.
[26] Jurado-Martin, I., M. Sainz-Mejias, and S. McClean, Pseudomonas aeruginosa: An audacious pathogen with an adaptable arsenal of virulence factors. International Journal of Molecular Sciences, 2021. 22(6): p.31-48.
[27] Gorniak, I., R. Bartoszewski, and J. Kroliczewski, Comprehensive review of antimicrobial activities of plant flavonoids. Phytochemistry, 2019. 18(1):p. 241-272.
[28] Lee, J.H., Y.G. Kim, and M.H. Cho, ZnO nanoparticles inhibit Pseudomonas aeruginosa biofilm formation and virulence factor production. Microbiological research, 2014. 169(12): p. 888-896.
[29] Sonnleitner, D. and C. Sommer, Approaches to inhibit biofilm formation applying natural and artificial silk-based materials. Materials Science and Engineering: C, 2021. 131: p.112-132.
[30] Prakash, H. and H. Bhojya, Synthesis of novel benzo[h]quinolines: Wound healing, antibacterial, DNA binding and in vitro antioxidant activity. European journal of medicinal chemistry, 2009. 44 (3): p. 981.

BIOGRAPHIES OF AUTHORS

Dr. Enass Jasim Waheed is Assist. Prof. at the College of Education for Pure Sciences, Ibn -Al-Haitham, University of Baghdad she obtained a doctor's degree in chemistry from College of Education for Pure Sciences, Ibn -Al-Haitham. 2016. Her areas of research are: Chemistry includes organic and inorganic aspects and includes the characterization of complexes and their applications. She can be contacted at email: enass.j.w@ihcoedu.uobaghdad.edu.iq